Information-Theoretic Detection of Motor Unit Activity in Hemiparetic sEMG Signal

Benedict King, *Student Member, IEEE,* Alexander Kenneth Clarke, *Student Member, IEEE,* Dario Farina, *Fellow, IEEE*

***Abstract*—This paper examines how Sliding Window Permutation Entropy (PE) can be used to detect the firing of Motor Units from single-channel Surface Electromyography (sEMG) signals. The algorithm is tested first on a generated synthetic signal with low MU numbers and varying noise (-20dB to 20dB Signal-to-Noise Ratio), and then on sEMG data from patients with Transverse Myelitis (TM) and Stroke patients. Compared to a current gold-standard for MU detection, the Matched Continuous Wavelet Transform (CWT), the PE algorithm consistently performs better in terms of robustness to noise (effective for signals up to -10dB SNR), and sensitivity to low MU numbers (able to detect single MUs from a single-channel signal, even at low SNRs).**

***Index Terms*—Motor unit, neural drive to muscle, permutation entropy, information theory**

Work supported by the EPSRC Centre of Excellence in Neurotechnology, European Research Council Synergy Grant Natural BionicS (810346)

Benedict King, D. Farina (d.farina@imperial.ac.uk) and A.K. Clarke (a.clarke18@imperial.ac.uk) are with the Department of Bioengineering, Imperial College London

I. Introduction

INTENSIVE task-directed physiotherapy is vital to improving functional outcomes after stroke[1][2]. Despite this access to physiotherapy is severely resource-constrained, meaning patients often do not get the required clinical focus to optimally recover[3]. One potential solution is to supplement physiotherapy with automated or patient-directed interventions, for example using a simple hand-held device to track movement and so control a game[4]. However, whilst sensitive to small motions, these devices fail when the patient has a complete paresis, meaning no movement at all can be generated. However, whilst these patients are unable to generate a functionally-meaningful force, they often continue to have detectable electromyography (EMG) signal under conscious control[5]. This suggests an alternative method of rehabilitation device control using a surface EMG (sEMG) based human-machine interface (HMI).

sEMG is a common clinical technique for diagnosing the causes for loss of motor function and for testing the efficacy of treatment strategies for patients with pre-diagnosed conditions [6]. While traditional EMG methods required intramuscular electrodes to be inserted into a patient's muscle fibres [7], the alternative method of surface electromyography (sEMG) has the advantages of being non-invasive and providing a more general overview of a muscle's electrical behaviour, but at the expense of signal quality [8]. Therefore an area of research has emerged, seeking new methods of extracting data from sEMG signals that can provide the same insight into muscular behaviour as the invasive EMG has done previously.

A common clinical use of both EMG and sEMG is for detecting the presence of functioning Motor Units (MUs) connecting to a region of muscle. For this purpose then, the signal analysis problem becomes a threshold one, with a result of on or off, depending on whether there are Motor Unit Action Potentials (MUAPs) present in the signal. Several methods have been proposed for this scenario, from simple single-threshold algorithms that are effective for low noise, high MU count signals [9], to more complex algorithms that can provide improved biases and classification accuracy for slightly higher noise signals [10]. Although these methods perform well for low noise and high MU count signals, because they share the common feature of taking a single-threshold from a filtered form of the original sEMG signal, they start to break down when the amplitude of the noise approaches that of the pure MUAP signal.

More recently, a novel approach has been to use machine-learning based algorithms such as neural network architectures to analyse single-channel, and often also multi-channel, sEMG signals [11], [12], [13]. These machine-learning approaches have the advantage of being better suited to classify different muscle movements from the signal rather than simply detect the presence of MUs, and they achieved high accuracy for many of the test signals, although the noise levels of the signals used were either low or undisclosed. These methods come at a cost

as well, which is the amount of prior training of the networks required. The network trained in [12] required a week of continuous computation after dimensionality reduction, and over two months before reducing dimensionality, on an 8 core CPU.

Information theoretic algorithms thus have the advantages over machine learning approaches of not needing model training, being often computationally faster, and being transparent in their decision process - in contrast to the *black-box* approach of many machine learning algorithms. Furthermore, the simplicity of the theory behind information theoretic algorithms gives confidence that they will be less sensitive to changes in signal forms such as amplitude and MUAP shape, and thus more robust as a detection method.

The information theoretic measure of entropy can be thought of as a measure of the disorder present in a time series. Thus an sEMG signal can be classified as MUs present versus not present depending on the amount of structure present in the signal. Several variations of entropy have been suggested as methods for biological signal analysis because of their intrinsic ability to distinguish random noise from structured signals, such as Sample Entropy (single and multi-scale) [14], and Lempel-Ziv Complexity [15]. However, one of the simplest and computationally fastest variants of entropy is the Permutation Entropy, as proposed by Bandt and Pompe [16].

Thus the purpose of this paper is to examine whether the permutation entropy of a single-channel sEMG signal can be used as a reliable and robust method for detecting motor unit presence, even in the high noise and low motor unit count scenarios that can be presented in sEMG signals.

II. Methods

In order to test the efficacy of the PE algorithm (as set out in part C), a current gold-standard for MU detection in sEMG signals, the Continuous Matched Wavelet Transform (described in part B), was used as a comparison. Both methods are tested on a biologically accurate synthetic sEMG signal so that factors such as SNR, MU number, and MU firing duration can be readily controlled. The process used to generate of this signal is outlined below in part A. Finally, part D outlines the threshold methods used to decide whether there is MU activity in a signal, based on its PE or CWT representation.

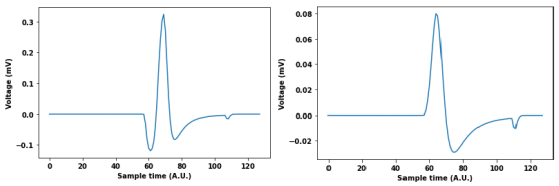

Fig. 1: Examples of two templates ($f_i(t)$) used to generate the synthetic sEMG signals.

A. Synthetic Signal Generation

As proposed in [12], the synthetic signal used to test the algorithms in this paper was generated by producing a true signal (one without noise) for a single MU, and then summing these signals over all of the MUs detectable from the sensor. For each single MU, the true signal consists of a repeating function template (sometimes referred to as the *prototype function*) convolved onto a binary spike train that represents the firing times of the MU. Mathematically, this is expressed as:

$$\text{MUAP}_i(t) = \sum_j f_i\left(t - \theta_{ij}\right) \tag{1}$$

where $f_i(t)$ is the ith MU's function template and θ_{ij} its spike train firing times. The values for θ_{ij} were produced by assuming that the time between successive firings of a single MU follow a Poisson distribution, i.e. $\theta_{i,j} = \theta_{i,j-1} + \delta$, for $\delta^{-1} \sim \text{Poisson}(\lambda)$ with λ the firing rate. Examples of two possible $f_i(t)$ templates that are commonly found in sEMG signals [17] are shown in Fig. 1.

If the true signal at the sensor is then the sum of the signals from each MU, then the true signal at the sensor becomes:

$$Y(t) = \sum_i \text{MUAP}_i(t) = \sum_i \sum_j f_i\left(t - \theta_{ij}\right) \tag{2}$$

In reality, any detected signal will have some amount of corrupting noise due to interference from other unrelated sources and imperfect sensors, and this noise is assumed to be additive, such that the actual detected signal at the sensor is:

$$S(t) = Y(t) + n(t) = \sum_i \sum_j f_i\left(t - \theta_{ij}\right) + n(t) \tag{3}$$

For the rest of the paper, this additive noise is assumed to be Gaussian, with a standard deviation σ_n that dictates the signal's Signal-to-Noise Ratio (SNR) through:

$$\text{SNR}_{\text{dB}} = 10\log_{10}\left(\frac{\sigma_S^2}{\sigma_n^2}\right) = 20\log_{10}\left(\frac{\sigma_S}{\sigma_n}\right) \tag{4}$$

B. Matched Continuous Wavelet Transform (CWT)

A method that has previously been shown to be effective at detecting MU presence in Surface EMG signals is the Matched Continuous Wavelet Transform [10], which assumes that the prototype function [see (1-3)] is the same for all MUs, but with amplitude and width scaling that is dependent on each MU. Consequently, the CWT signal can be expressed as:

$$S_{\text{CWT}} = \bar{S}(t) = \sum_i \sum_j \beta_i f\left(\frac{t-\theta_{ij}}{\alpha_i}\right) + n(t) \quad (5)$$

for β_i and α_i the amplitude and width scaling of $f(t)$.

The definition for CWT is then as follows [18]:

$$\text{CWT}(a,t) = \frac{1}{\sqrt{a}} \int_{-\infty}^{\infty} \bar{S}(t) W^*\left(\frac{\tau - t}{a}\right) d\tau \quad (6)$$

where $W(t)$ is the *mother wavelet* and a its scaling parameter. If the prototype function is the same as the mother wavelet, $f(t) = W(t)$, then the CWT effectively picks out the functions $f(t)$ within the noisy signal $S(t)$ that have the same scaling parameter as the CWT (i.e. where $\alpha_i = a$). Thus for different values of a, $\text{CWT}(a,t)$ has maxima at different times, corresponding to the presence of MUAPs of different scales in $S(t)$. [10] proposes using a bank of filters, each corresponding to a unique a, to resolve this issue. In this case, the filtered signal is the maximum of a bank of CWTs with different scaling factors, $\{a_k\}$:

$$\eta(t) = \max_{a \in \{a_k\}} \text{CWT}(a,t) \quad (7)$$

A choice of mother wavelet and scale factors must therefore be chosen that suitably represent the function templates present in sEMG signals. Examples of suitable templates [17] can be seen in Fig. 1, with a Ricker Wavelet [19] (similar to the left-hand plot) given by:

$$W\left(\frac{t}{a}\right) = \frac{1}{\sqrt{3a}\pi^{1/4}} \left(1 - \left(\frac{t}{a}\right)^2\right) \exp\left(-\frac{t^2}{2a^2}\right) \quad (8)$$

and a first order Hermite Rodriguez [20] function (similar to the right-hand plot) given by:

$$W\left(\frac{t}{a}\right) = HR_1\left(\frac{t}{a}\right) \exp\left(-\frac{t^2}{a^2}\right) = 2\left(\frac{t}{a}\right) \exp\left(-\frac{t^2}{a^2}\right) \quad (9)$$

For the remainder of the paper, the Ricker Wavelet [see (8)] is used in CWT filtering, as it performed best on the generated synthetic signal. According to previous sEMG signal studies and measurements from experimental sEMG data [10], [21], the period of MUAPs tends to lie in the 5-40 ms range. Therefore the scaling factors used for the bank of CWTs are $\{a_k\} = \{5, 10, 15, 20, 25, 30, 35, 40, 45\}$ ms.

C. Sliding Window Permutation Entropy (PE)

In contrast to the CWT, the PE method makes no assumptions about the underlying signal, except that it is discrete, and will have more structure, and hence lower entropy, when there is a MUAP present versus when the signal is purely noise. For the sliding window PE method, the signal $S(t)$ of length L is split into sliding windows of length N, each denoted s_i, $i = 1, 2, ..., (L+1-N)$. The following algorithm, as proposed in [16], is then implemented to return the permutation entropy of each window, s_i:

1) The sliding window signal of length N is further split into sliding window batches of length m, where m is the *embedding dimension*, such that there are $(N+1-m)$ m-length batches.
2) Each element in the m-length batches takes a value, 1 to m, based on its size relative to the other elements in the batch. If two or more elements are equal, the elements that appear later in the batch are allocated higher values. For example, if $m = 4$, a batch with elements (5,1,3,1) would become (4,1,3,2). This new array will be referred to here-on-through as a *motif*.
3) There are $m!$ permutations of a motif, and thus each motif is designated a number, 1 to $m!$, such that each s_i is now represented by a series of $(N+1-m)$ motif identifiers, denoted $M(s_i)$. The value of each identifier is arbitrary, so long as it represents a unique motif. A diagram showing steps 1 through to 3 can be seen in Fig. 2.
4) A frequency distribution $\pi_i(j)$ is introduced and defined as the frequency of motif j in sliding window s_i. For large enough sliding window length, N, the frequency distribution tends to a probability distribution, and so $\pi_i(j)$ becomes the probability of motif j in sliding window s_i. Mathematically this is expressed as:
$$\pi_i(j) = \frac{\{\#j \in M(s_i)\}}{N+1-m} \quad (10)$$
5) From here the permutation entropy (in Bits) of each sliding window s_i can be defined in the usual way as:
$$H_2^i(\pi_i) = -\sum_{j=1..m!} \pi_i(j) \log_2\left[\pi_i(j)\right] \quad (11)$$

The entropy in (11) is bounded by $0 \leq H_2^i \leq \log_2(m!)$, and so the normalised permutation entropy is thus defined as:

$$\hat{H}_2^i = \frac{H_2^i}{\log_2(m!)} \tag{12}$$

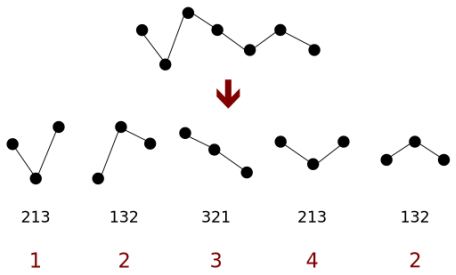

Fig. 2: An example of an $N = 7$ sliding window, s_i, from a signal $S(t)$, being reduced to an array of motif identifiers with embedding dimension $m = 3$. Here, $M(s_i) = \{1, 2, 3, 4, 2\}$. Motif 5: 312, is not present in this sliding window, and thus the motif probability distribution is not quite uniform, so the normalised entropy, although high, will not be a maximum.

The Sliding Window Permutation Entropy (in bits) is then the series $\hat{H} = \{\hat{H}_2^1, \hat{H}_2^2, ..., \hat{H}_2^{(L-N)}, \hat{H}_2^{(L+1-N)}\}$, and can be used as a dynamic measure of the disorder, and by extension the unpredictability, of the time series being analysed. As noise, particularly Gaussian noise, is expected to be less ordered and predictable then a series of MUAPs, it is hoped that the presence of MUs firing in an sEMG signal can be identified by a drop in the signal's PE.

D. Post-processing and Threshold Methods

1) Standard Deviation Threshold: If the firing of MUs is to be recognised as a drop in the PE, then there must be a method of detecting when the PE value goes below a threshold. The simplest method to do this, and one that is used often in biological signal analysis [9], [10], is to just predefine a value for the PE below which the MUs are predicted to be firing. This raises the question of how to choose such a value, particularly if the range of entropies vary greatly between different sEMG signals. A common way around this is to assume that some early part of the signal is pure noise, and to define the threshold, T, as:

$$T = \mu_N - \gamma * \sigma_N \tag{13}$$

for μ_N and σ_N the mean and standard deviation of the first part of $\hat{H}$, assumed to represent pure noise, and γ a multiplicative factor.

2) Chi-Square Threshold: A disadvantage of the standard deviation threshold is its sensitivity to erroneous fluctuations in the PE, as the slightest fall in below T will be identified as MU presence, regardless of the duration of the drop. This problem of false positive detection is common to all threshold methods, but as proposed in [22], the issue can be improved by considering the sum of squared consecutive points in the series, such that any isolated erroneous fluctuation may be counteracted by an adjacent non-erroneous value.

Taking the PE series found using the method in part C, it is useful, for reasons explained shortly, to normalise the series to a Z-statistic, with μ_N and σ_N found in a similar fashion to before, from a part of $\hat{H}$ assumed to represent pure noise:

$$Z_i = \frac{\hat{H}_2^i - \mu_N}{\sigma_N} \tag{14}$$

The sum of k consecutive squared values of is then expressed as:

$$\begin{aligned} X_i &= \sum_{j=ki+1-k}^{ki} Z_j^2 \\ \text{len}(X) &= \left\lfloor \frac{\text{len}(Z)}{k} \right\rfloor \end{aligned} \tag{15}$$

Choosing a high value of k reduces the false positive rate, as erroneous fluctuations are more likely to be cancelled in a sum of more values, but the cost of a high k value is a higher false negative rate due to a detection lag introduced when the series is shrunk by a factor of k. Therefore a compromise is required, and similarly to in [22], the value chosen for this paper is $k = 2$.

Due to the normalisation of $\hat{H}$ to a series of Z-statistics, any significant fall in the PE at point $\hat{H}_2^i$ is now represented by a large negative Z_i. Therefore, a prolonged drop is represented by consecutive large negative Z-statistics, and thus a large positive value of X. This leads to a choice of threshold, ζ, such that the section of the PE series $\{\hat{H}_2^{ki+1-k}, ..., \hat{H}_2^{ki}\}$ is said to represent MUs firing if $X_i \geq \zeta$.

A choice for ζ that maximises the true positive rate (tpr) to false positive rate (fpr) ratio can be found by repeated testing with varying values for ζ. However, an estimate for this suitable choice can be found analytically by assuming that the entire sEMG signal is noise, and then finding a value for ζ that makes the probability of

false positive detection below 0.05, given that $\hat{H}$ (and thus X) represents a pure noise signal:

$$P(X_i \geq \zeta | S(t) = \text{noise}) \leq 0.05 \tag{16}$$

If the sEMG signal is purely noise then, as the noise is assumed to be normally distributed, $\hat{H}$ is also normally distributed, and thus X is distributed via a χ^2-distribution, with k degrees of freedom. Therefore, taking $k = 2$:

$$P(X \geq \zeta | X \sim \chi^2(\nu = 2)) = \frac{1}{2} \int_{\zeta}^{\infty} \exp\left(-\frac{x}{2}\right) dx \tag{17}$$

Therefore, combining (17) with (16), $\zeta \approx 6$.

III. Results and Discussion

In order to finely control the characteristics of the sEMG signal such as noise and MU number, the generated signal as described in section 2.1 was used first to test the three algorithm combinations. Another advantage of this is that multiple unique signals with the same noise and MU characteristics can be quickly and easily generated by exploiting the random nature of the choice of template shape and the time between spikes in the MU spike trains. Real patient sEMG data from stroke patients were then used to test the algorithms applicancy to clinical settings.

A. Using a Generated Synthetic Signal

1) Varying MU Number: Fig. 3 shows how the PE algorithm performed when tested on signals with varying number of MUs. The raw signal was pre-filtered using a Gaussian filter, with a kernel width of 9 and standard deviation of 3. The algorithm was then tested with a window size of 1000 *ms* and sampling frequency of 2048 *Hz*, for signal to noise ratios of 10 *dB* and 30 *dB*. As the plot demonstrates, the PE algorithm performs sufficiently well to detect MU presence with as little as a single MU, and as expected, its ability to differentiate signal from noise continues to improve with MU number increase. However, the rate of improvement is greatest as the MU numbers increase from 1 through to 5 MUs, which is reassuring for the clinical purpose of this paper, as functioning MU numbers are often below 5 in the sEMG signals of patients suffering from neurological impairment.

The standard errors on the bars in Fig. 3 reflect the fact that, even for constant noise and MU number, the PE of the signal can vary due to variations of template shape and stochastically generated spike train timings, which reflects to an extent the natural variation found between different patients' sEMG signals.

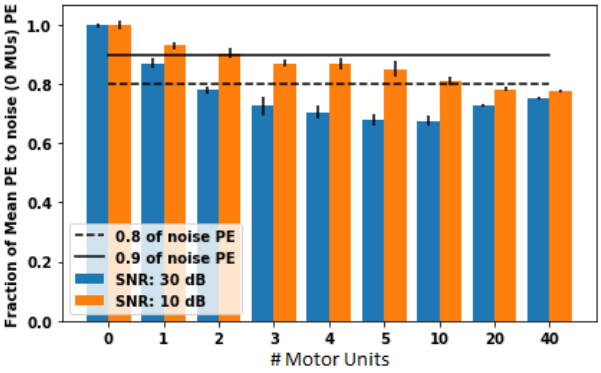

Fig. 3: The performance of the PE algorithm on a varying number of MUs. Even for low MU numbers there is clear distinction between the noise PE and the PE of the generated sEMG signal. The error bars represent the standard error for 10 repeated measurements on unique signals.

2) On-Off Signal And Real-Time Detection: For section 3.1.2 and 3.1.3 an alternative 20 second synthetic signal was generated, with a sampling frequency of 2048 *Hz*, consisting of Gaussian noise of a set SNR with 1 MU firing between 4 and 8 seconds and 2 MUs firing between 12 and 16 seconds.

With this new signal the temporal sensitivity of the PE algorithm can be investigated for varying SNR, and the efficacy easily visualised - a significant bench-mark would be if the PE algorithm is able to correctly detect MU presence at an SNR low enough that it is not obvious in a simple visual check. However, even for signals that have clear visual MU presence, an automated detection process is still very relevant, as it could allow for continual monitoring of motor function in a clinical setting.

Fig. 4 shows six plots for the new synthetic signal for varying SNR from -20 to 20 *dB* with a step-plot superimposed that has value zero when no MUs are detected from the PE + χ^2 algorithm, and a non-zero value when MUs are detected. The plots demonstrate the ability that the algorithm has to detect MUs from signals of noise levels down to -20 *dB*, albeit with a high false negative probability. However, when the noise levels are above 0 *dB*, which is reasonable for even low resolution sEMG signals taken in a clinical setting, the PE method is able to effectively determine the difference between MU

presence and their absence, even in the 1 MU case.

In the legend of each plot the two biases are given as the time difference between the true MU onset and the detected onset for the single MU case and the two MU case respectively, where a negative value of the bias reflects a delay between actual onset and subsequent detection. In all six cases the bias is very low, and comparable to the biases obtained from the CWT + σ algorithm investigated in [10], even for the higher noise signals. Coupled with the fast computational speed due to the simplicity of the PE algorithm, this low bias allows for live-time onset/offset detection, and the possibility for continual recording of muscle MU activity that is robust to noise and sensitive to low MU numbers.

3) Robustness to Noise: From Fig. 4 it appears that the PE algorithm performs well for noises greater than 0 *dB*, but its performance with varying noise can be explicitly quantified by the use of Receiver Operating Characteristic curves (ROC curves). The relationships between True Positive probability and False Negative Probability were therefore calculated for different choices of threshold sensitivity (i.e. different choices for the value of χ) and are plotted in Fig. 5 (black line) for varying SNR. The results in Fig. 5 are for 5 unique signals generated in the same format as described in section 3.1.2. The higher the True Positive Probability relative to the False Positive Probability, the better an algorithm performs at detecting MU presence whilst not being too sensitive that MU firing is detected at times where no MUs are present. Therefore, from Fig. 5, the PE + χ^2 method is shown to perform better than both the CWT + σ and unfiltered + χ^2 methods for all SNRs, with almost ideal performance for 10 and 20 *dB*.

REFERENCES

[1] G. Kwakkel, R. van Peppen, R. C. Wagenaar, S. W. Dauphinee, C. Richards, A. Ashburn, K. Miller, N. Lincoln, C. Partridge, I. Wellwood, and P. Langhorne, "Effects of augmented exercise therapy time after stroke," *Stroke*, vol. 35, pp. 2529–2539, Nov. 2004.

[2] K. R. Lohse, C. E. Lang, and L. A. Boyd, "Is more better? using metadata to explore dose–response relationships in stroke rehabilitation," *Stroke*, vol. 45, pp. 2053–2058, July 2014.

[3] J. Bernhardt, J. Chan, I. Nicola, and J. Collier, "Little therapy, little physical activity: Rehabilitation within the first 14 days of organized stroke unit care," *Journal of Rehabilitation Medicine*, vol. 39, no. 1, pp. 43–48, 2007.

[4] P. Rinne, M. Mace, T. Nakornchai, K. Zimmerman, S. Fayer, P. Sharma, J.-L. Liardon, E. Burdet, and P. Bentley, "Democratizing neurorehabilitation: How accessible are low-cost mobile-gaming technologies for self-rehabilitation of arm disability in stroke?," *PLOS ONE*, vol. 11, p. e0163413, Oct. 2016.

[5] E. Loopez-Larraz, N. Birbaumer, and A. Ramos-Murguialday, "A hybrid EEG-EMG BMI improves the detection of movement intention in cortical stroke patients with complete hand paralysis," in *2018 40th Annual International Conference of the IEEE Engineering in Medicine and Biology Society (EMBC)*, IEEE, July 2018.

[6] Y. Wu, M. ngeles Martnez Martnez, and P. O. Balaguer, "Overview of the application of EMG recording in the diagnosis and approach of neurological disorders," in *Electrodiagnosis in New Frontiers of Clinical Research*, InTech, May 2013.

[7] "Electromyography (emg)," in *Mayo Clinic*, Mayo Clinuc, 2019.

[8] S. L. Pullman, D. S. Goodin, A. I. Marquinez, S. Tabbal, and M. Rubin, "Clinical utility of surface EMG: Report of the therapeutics and technology assessment subcommittee of the american academy of neurology," *Neurology*, vol. 55, pp. 171–177, July 2000.

[9] L. Hedman, M. Rogers, Y.-C. Pai, and T. Hanke, "Electromyographic analysis of postural responses during standing leg flexion in adults with hemiparesis," *Electroencephalography and Clinical Neurophysiology/Electromyography and Motor Control*, vol. 105, pp. 149–155, Apr. 1997.

[10] A. Merlo, D. Farina, and R. Merletti, "A fast and reliable technique for muscle activity detection from surface EMG signals," *IEEE Transactions on Biomedical Engineering*, vol. 50, pp. 316–323, Mar. 2003.

[11] B. Karlık, "Machine learning algorithms for characterization of EMG signals," *International Journal of Information and Electronics Engineering*, vol. 4, no. 3, 2014.

[12] U. C. Allard, C. L. Fall, A. Drouin, A. Campeau-Lecours, C. Gosselin, K. Glette, F. Laviolette, and B. Gosselin, "Deep learning for electromyographic hand gesture signal classification by leveraging transfer learning," *CoRR*, vol. abs/1801.07756, 2018.

[13] R. Chowdhury, M. Reaz, M. Ali, A. Bakar, K. Chellappan, and T. Chang, "Surface electromyography signal processing and classification techniques," *Sensors*, vol. 13, pp. 12431–12466, Sept. 2013.

[14] M. Costa, A. L. Goldberger, and C.-K. Peng, "Multiscale entropy analysis of biological signals," *Physical Review E*, vol. 71, Feb. 2005.

[15] M. Aboy, R. Hornero, D. Abasolo, and D. Alvarez, "Interpretation of the lempel-ziv complexity measure in the context of biomedical signal analysis," *IEEE Transactions on Biomedical Engineering*, vol. 53, pp. 2282–2288, Nov. 2006.

[16] C. Bandt and B. Pompe, "Permutation entropy: A natural complexity measure for time series," *Physical Review Letters*, vol. 88, Apr. 2002.

[17] *Aminoff's Electrodiagnosis in Clinical Neurology*. Elsevier, 2012.

[18] P. S. Addison, "Introduction to redundancy rules: the continuous wavelet transform comes of age," *Philosophical Transactions of the Royal Society A: Mathematical, Physical and Engineering Sciences*, vol. 376, p. 20170258, July 2018.

[19] Y. Wang, "The ricker wavelet and the lambert w function," *Geophysical Journal International*, vol. 200, pp. 111–115, Nov. 2014.

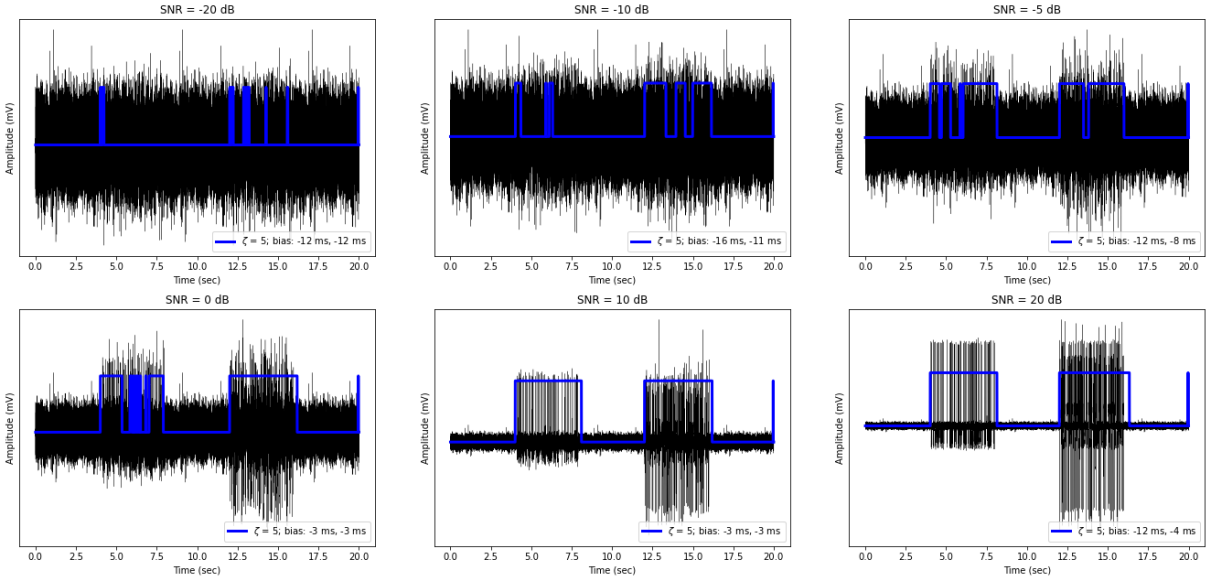

Fig. 4: Plots showing the time delay for the on/off triggering using the PE algorithm with χ^2 post-processing on the synthetic signal. The window size used was 500 *ms* and the embedding dimension was $m = 3$. For the post-processing, the value of χ was 5 in each case.

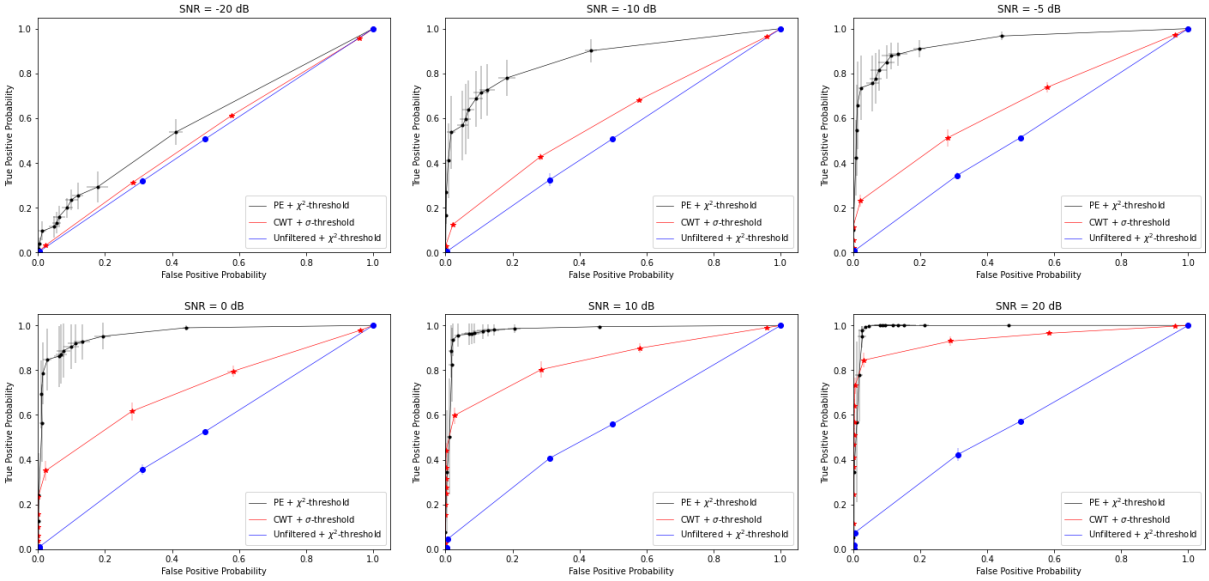

Fig. 5: ROC curves comparing the PE algorithm with χ^2-threshold post-processing to the CWT algorithm using standard deviation threshold post-processing. The algorithms were tested on 5 unique randomly generated synthetic signals using the method outlined in Section 2.1, again with a window size for the permutation entropy of 500 *ms* and embedding dimension of 3.

[20] L. L. Conte, R. Merletti, and G. Sandri, “Hermite expansions of compact support waveforms: applications to myoelectric signals,” *IEEE Transactions on Biomedical Engineering*, vol. 41, no. 12, pp. 1147–1159, 1994.

[21] I. Rodriguez-Carreno, L. Gila-Useros, and A. Malanda-Trigueros, “Motor unit action potential duration: Measurement and significance,” in *Advances in Clinical Neurophysiology*, InTech, Oct. 2012.

[22] P. Bonato, T. D'Alessio, and M. Knaflitz, “A statistical method for the measurement of muscle activation intervals from surface myoelectric signal during gait,” *IEEE Transactions on Biomedical Engineering*, vol. 45, pp. 287–299, Mar. 1998.